Proc. Nat. Acad. Sci. USA
Vol. 69, No. 11, pp. 3142–3145, November 1972

Electron Paramagnetic Resonance of Nitrogenase and Nitrogenase Components from *Clostridium pasteurianum W5* and *Azotobacter vinelandii OP*

(iron–sulfur proteins/ferredoxins/electron transfer/nitrogen fixation/Mg·ATP)

W. H. ORME-JOHNSON*†, W. D. HAMILTON*, T. L. JONES†, M.-Y. W. TSO†, R. H. BURRIS†, V. K. SHAH‡, AND W. J. BRILL‡

* Institute for Enzyme Research, † The Department of Biochemistry, and ‡ The Department of Bacteriology, College of Agricultural and Life Sciences, University of Wisconsin, Madison, Wis. 53706

Contributed by R. H. Burris, August 28, 1972

ABSTRACT **The electron paramagnetic resonance of nitrogenase components, separately and together with the other reactants in the nitrogenase system (namely, reductant and Mg·ATP), have been examined at low temperatures (<20°K). The MoFe protein, component I or molybdoferredoxin, in the oxidized (but not oxygen-inactivated) state yields signals with g-values of 4.3, 3.7, and 2.01, and when reduced has no observable electron paramagnetic resonance. The Fe protein, component II, or azoferredoxin, yields a signal with g-values of 2.05, 1.94, and 1.89 in the reduced state that is converted by Mg·ATP into an axial signal with g-values near 2.05 and 1.94, and a second split signal near g = 4.3. The Fe protein has no definite electron paramagnetic resonance in the oxidized (not oxygen-denatured) state under these conditions. The Mg·ATP complex of reduced Fe protein reduces the MoFe protein, whereas dithionite alone does not reduce the MoFe protein. Reoxidation of the system by substrate leads to disappearance of the Fe protein signal and the reappearance of the MoFe protein signal. Thus Mg·ATP, which is hydrolyzed during substrate reduction, converts the Fe protein to a reductant capable of transferring electrons to MoFe protein, after which substrate reduction occurs.**

In the past few years, the art of purifying the protein components of nitrogenase has progressed to the stage where essentially homogeneous preparations of the MoFe protein (component I, molybdoferredoxin) and the Fe protein (component II, azoferredoxin) have been described from *Azotobacter vinelandii* (1–3), *Clostridium pasteurianum* (4–7), *A. chroococcum* (8), and *Klebsiella pneumoniae* (9). The principal difficulty has been that the proteins are rapidly inactivated by oxygen. We, as well as others, have described the electron paramagnetic resonance (EPR) signals obtained from the MoFe protein at low (<30°K) temperatures, both *in vivo* (10) and *in vitro* (10–12). Because these signals appear to arise from transition metal complexes, and because it has been generally anticipated that the transition metal complexes in nitrogenase are intimately involved in the six-electron reduction of N_2 to NH_3 (e.g., refs. 11–13), we undertook to develop techniques for examining reaction mixtures under anaerobic conditions at equilibrium and in steady-states, as a prerequisite to kinetic studies of electron transfers in nitrogenase. In the present report, we describe EPR signals obtained from MoFe and Fe proteins, separately and together, and the effect of the other two substances required for nitrogen fixation (Mg·ATP and low-potential reductant) on these signals. From these experiments, we assign apparent relative oxidation states to the components under the various conditions, and discuss possibilities for the electron fluxes in nitrogenase during reduction of substrates.

Abbreviation: EPR, electron paramagnetic resonance.

METHODS

EPR Spectroscopy was performed with a modified Varian machine (14) operating at microwave frequency of 9.2 GHz, and with modulation frequency of 100 kHz. Sample temperatures were maintained at 13 ± 0.1°K with a stream of helium boiloff gas, and were monitored with a carbon-resistance thermometer 1-cm upstream from the sample.

Preparation of Samples. The EPR tubes used were a form of Thunberg tube (15), arranged so that the EPR tube (5-mm outer diameter) itself was sealed to the upper chambers by way of a 7/15 standard taper joint. A stopcock was attached to the sidearm of the upper chamber with a rubber serum stopper sealed to the outlet of the stopcock. A second stopcock connected the apparatus to an evacuation and gassing manifold. The vacuum system included a liquid-nitrogen-cooled trap, and the inert gas (argon) was scrubbed to below 1 ppm O_2 by passage over H_2-activated BTS catalyst (Kontes Glass Co.) at 200°C. Oxygen in the inert gas stream was measured by the method of Sweetser (16). The serum cap and stopcock on the sidearm of the Thunberg–EPR tube allows one to degas the system empty, with five or more cycles of gassing and evacuation, with the sidearm stopcock open. After this, oxygen-sensitive protein solutions can be transferred with a syringe through the serum cap into the EPR apparatus, which is left under a positive pressure of argon. The sidearm stopcock then is closed and the solutions in the apparatus can be subjected to futher cycles of evacuation and gas flushing without danger of pulling air into the apparatus through the pierced septum. When appropriate, buffers, ATP–phosphocreatine–creatine kinase mixture, and methyl viologen were introduced into the apparatus and degassed, after which the $Na_2S_2O_4$ solution and protein solutions were added to the sidearm. After further flushing, to reduce the effect of any oxygen added during the transfers, the mixture was shaken down into the evacuated EPR tube, and the sample was frozen by immersion in a stirred isopentane bath maintained at 130°K. According to control experiments in which a thermocouple was placed in an EPR tube with buffer, freezing took place in about 3 sec. The sample tubes were then

immersed in liquid nitrogen until EPR spectroscopy could be performed.

Nitrogenase Components. These proteins were prepared as described elsewhere (ref. 7, also Shah and Brill, modification of the methods of ref. 1) and had the following specific activities [expressed as nmol of acetylene reduced per min per mg of protein, in the standard assay (7)]: *C. pasteurianum* MoFe protein, 1400; Fe protein, 1200—*A. vinelandii*, MoFe protein 1600; Fe protein, 1500. Protein concentrations were determined by the Goa modification of the biuret reaction (17).

Other Reagents. NaATP, phosphocreatine, creatine kinase, methyl viologen, and Tris base were obtained from Sigma Chemical Co., St. Louis, Mo; sodium dithionite was obtained from Hardman and Holden, Ltd., Manchester. Except as noted, an ATP-generating system consisting of 5 mM ATP, 6 mM $MgCl_2$, 40 mM phosphocreatine, and 0.2 mg of creatine kinase per ml was present in the reaction mixtures.

RESULTS AND DISCUSSION

EPR of the Fe protein and the effect of Mg·ATP

Spectra of the Fe protein from *C. pasteurianum* in the presence of 5 mM $Na_2S_2O_4$ are shown in Figs. 1*a* and 2*b*. The portion of the spectrum near g = 2 with g-values of 2.05, 1.94 (midpoint), and 1.88, resembles the spectrum of reduced spinach ferredoxin (21). Identical g-values are found with the Fe protein from *A. vinelandii*, and Eady *et al.* (9) report similar values for the corresponding protein of *K. pneumoniae*. When the signal is quantitated by comparison of its double integral to that obtained from a standard Cu·EDTA solution, 0.79 spins per four iron atoms (calculated from the iron content of the sample, ref. 18) are found when the spectra are obtained at 13°K, and at nonsaturating microwave powers (i.e., <10 mW). The signal rapidly broadens and disappears at temperatures above 20°K. A signal is seen in various amounts near g = 4, depending on the preparation. It may represent denatured protein or adventitiously bound iron.

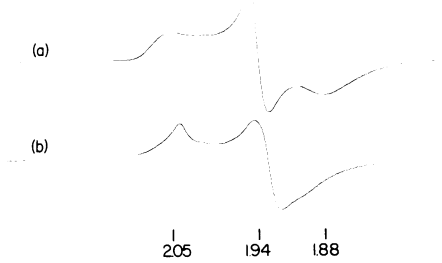

FIG. 1. EPR of the Fe protein of *C. pasteurianum* nitrogenase, with and without Mg·ATP. The samples contained 8.8 mg of Fe protein per ml (160 μM, based on a molecular weight of 55,000), as well as 2 mM sodium dithionite and 25 mM Tris·HCl (pH 8.0). (*a*) contains the described mixture; (*b*) in addition contains 1 mM ATP and 2 mM $MgCl_2$. The conditions of EPR spectroscopy were: microwave frequency, 9.18 GHz; microwave power, 9 mW; modulation frequency, 100 KHz; modulation amplitude, 12 G; magnetic-field sweep rate, 400 G per min; time constant, 0.25 sec; sample temperature, 13°K. The g-values indicated on the *abscissa* were calculated from magnetic-field positions derived from a proton NMR probe next to the cavity, and klystron frequencies obtained with a counter. The ordinates are an arbitrary function of the first derivative of the microwave absorption with respect to the magnetic field.

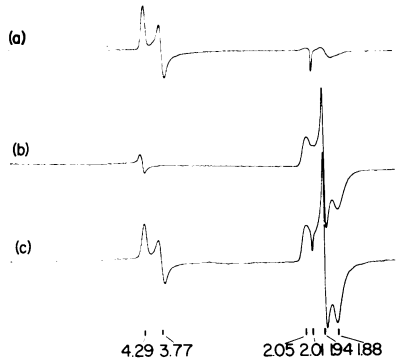

FIG. 2. EPR of the components of *C. pasteurianum* nitrogenase, in the absence of Mg·ATP. Proteins were placed in anaerobic EPR tubes and quick-frozen as described in *Methods*. In addition to the proteins, the solutions contained 5 mM $Na_2S_2O_4$ and 25 mM Tris·HCl (pH. 8.0). Conditions of EPR spectroscopy: microwave frequency, 9.17 GHz; microwave power, 2.7 mW; modulation frequency, 100 KHz; modulation amplitude, 6 G; magnetic-field sweep rate, 1000 G per min; time constant, 0.25 sec; sample temperature, 13°K. The g-values indicated on the *abscissa* were calculated from magnetic-field positions derived from a proton NMR probe next to the cavity and klystron frequencies determined with a counter. The ordinates are an arbitrary linear function of the first derivative of the microwave absorption with respect to the field; amplifier gains are the same for each spectrum. (*a*) 10 mg of MoFe protein per ml [48 μM based on a molecular weight of 210,000]; (*b*) 10 mg of Fe protein per ml [182 μM based on a molecular weight of 55,000]; (*c*) MoFe protein (10 mg/ml) with Fe protein (10 mg/ml).

Mg·ATP has been reported to bind to the Fe protein (19). When 1 mM Mg·ATP and 10 mg of Fe protein of *C. pasteurianum*/ml [182 μM, based on a molecular weight of 55,000 (12)] are present together, the EPR spectrum changes to that seen in Fig. 1*b*, where the shape has changed to a more nearly axial form. The integrated intensity in the region of g = 2 declined by 22%. At the same time (Fig. 3*b*), a split signal near g = 4.3 is seen in the Mg·ATP–Fe protein sample. This signal probably represents a second environment of iron

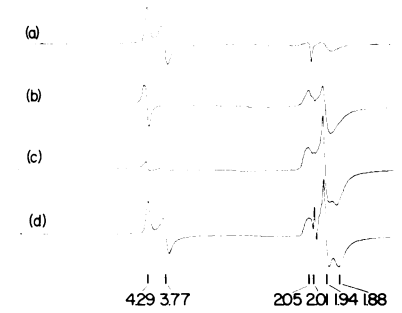

FIG. 3. EPR of the components of *C. pasteurianum* nitrogenase, in the presence of Mg·ATP. Conditions of EPR spectroscopy were as in Fig. 2. Each sample contained an ATP-generating system (see *Methods*) to maintain the Mg·ATP concentration near 5 mM. (*a*) 10 mg of MoFe protein per ml, plus 5 mM $Na_2S_2O_4$; (*b*) 10 mg of Fe protein per ml, plus 5 mM $Na_2S_2O_4$; (*c*) the two proteins, 10 mg of each per ml (i.e., at a molar ratio of 1:4; see Fig. 2) $Na_2S_2O_4$, frozen 45 sec after mixing; (*d*) same as (*c*), except that 0.5 mM $Na_2S_2O_4$ was initially present, along with 40 μM methylviologen, and incubation after mixing and before freezing was for 90 sec, at which time the bluish cast of reduced viologen was no longer visible.

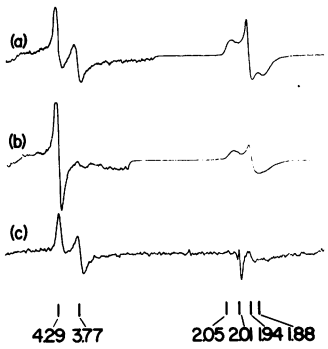

FIG. 4. EPR of components of *C. pasteurianum* nitrogenase mixed at a ratio of 1:16 (MoFe protein:Fe protein, see Fig. 2). Conditions of EPR spectroscopy were as in Fig. 2. (*a*) 2.5 mg of MoFe protein per ml, 10 mg of Fe protein/ml, and 5 mM $Na_2S_2O_4$; no ATP-generating system was added; (*b*) same as (*a*), but including the ATP-generating system (5 mM Mg·ATP). The sample was frozen 45 sec after mixing; (*c*) same as (b), but the $Na_2S_2O_4$ concentration was decreased to 0.5 mM and 40 μM methylviologen was present. The sample was incubated for 15 min before quick-freezing. Note that the final amplifier gain of the left halves of (*a*) and (*b*) and all of (*c*) were increased by 10-fold.

in the Fe protein, created by the interaction with Mg·ATP. The Fe protein, when titrated with Mg·ATP, changes from the spectrum of Fig. 1*a* to that of Fig. 1*b*, with intermediate states being apparent mixtures of two limiting species (M.-Y. Tso, R. H. Burris, and W. H. Orme-Johnson, unpublished observations).

EPR of the MoFe protein

Spectra of the purified MoFe protein of *A. vinelandii* show g-values at 4.3, 3.65, and 2.01 (10). Fig. 2*a* shows the spectrum of the MoFe protein of *C. pasteurianum* in the presence of 5 mM $Na_2S_2O_4$; there appear g-values at 4.29, 3.77, and 2.01. The signal near g = 1.94 is present in variable amounts in spectra of these preparations, and according to Dalton and Mortenson (12) represents an impurity, as we previously pointed out is the case in some MoFe preparations from *A. vinelandii* (10). If this signal arises from a protein of the ferredoxin type, it can be estimated by comparison to the Fe protein signal that it represents <10 mol percent of the MoFe protein represented in Fig. 2*a*.

No change was seen in the *shape* of the signal from the MoFe protein when Mg·ATP was added to a concentration of 5 mM (Fig. 3*a*), in contrast to the response of the Fe protein. The signal we identify with the MoFe protein does decline by 26% in overall height with added Mg·ATP, while the amplitude of the signal at g = 1.94 remains constant. Therefore, although the MoFe protein does not appear to *bind* Mg·ATP (19), it does respond to the presence of Mg·ATP under these conditions.

EPR of the MoFe and Fe proteins together, and the effect of Mg·ATP and reducing equivalents

When the MoFe and Fe proteins of *C. pasteurianum* are mixed in the absence of Mg·ATP, the EPR spectrum of the MoFe protein declines by 16%, and the signal due to the Fe protein narrows with an accompanying increase in signal height, as shown in Fig. 2*c*. The g = 2.01 portion of the MoFe protein signal can still be seen as a sharp indentation in the low-field side of the Fe protein signal, and there is no apparent trace of either the g = 4.3 signal originally present from the Fe protein alone nor of the g = 1.94 signal from the MoFe protein alone.

Upon the addition of Mg·ATP, the oxidation of dithionite commences (20). The present experiments were performed under argon (an atmosphere of N_2 gives the same picture), so that proton reduction was occurring in the sample whose spectrum is shown in Fig 3*c*, prior to freezing of the sample, about 1 min after mixing. In this case, where the MoFe protein–Fe protein molar ratio is 1:4, and where Mg·ATP (5 mM), an ATP-generating system and 5 mM $Na_2S_2O_4$ are initially present, a steady-state is reached in which the MoFe protein signal has declined by 92%, and in which the Fe protein signal appears to be a mixture of the signals of the Mg·ATP complex and free Fe protein. A second experiment was performed in which 40 μM methylviologen was present as an indicator of the presence of dithionite, and a limiting amount of (0.5 mM) $Na_2S_2O_4$ was added. After mixing, the solution was allowed to remain unfrozen until the bluish cast imparted by the methylviologen cation radical had disappeared (about 90 sec), whereupon the sample was frozen. The EPR spectrum of this sample is shown in Fig. 3*d*. The signal at g = 2 indicated that the methylviologen was not completely oxidized again, but the signal of the MoFe protein returned to 68% of its original size. A further experiment was performed with a molar ratio of MoFe protein to Fe protein of 1:16. When excess $Na_2S_2O_4$ was present, the signal of the MoFe protein declined by >90% (Fig. 4*b*). When limiting amounts of $Na_2S_2O_4$ and methylviologen were present, and the sample was allowed to stand for about 15 min to exhaust the dithionite completely, the spectrum in Fig. 4*c* was recorded, in which the signal of the MoFe protein has regained the amplitude it had before $Na_2S_2O_4$ was added to the system, whereas the signal of the Fe protein completely disappeared (note that the right-hand side of Fig. 4*c* was recorded at ×10 the gain of Fig. 4*b*). In Fig. 4*b*, most of the molecules of Fe protein appeared to be in a complex with Mg·ATP. This is reasonable because the Fe protein was present in large excess.

A series of EPR spectral changes similar to those described above occurs when lower concentrations of *C. pasteurianum* nitrogenase components are used. We have also observed the same features in experiments in which MoFe and Fe proteins from *A. vinelandii* were used together. The EPR of a series

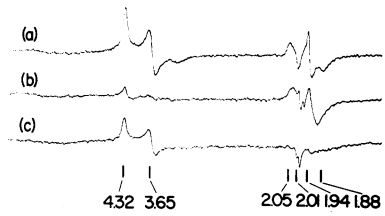

FIG. 5. EPR of components of *A. vinelandii* nitrogenase, mixed at a ratio of about 1:4 (MoFe protein:Fe protein). Conditions of EPR spectroscopy were the same as Fig. 2. (*a*) 4 mg of MoFe protein per ml, 3.2 mg of Fe protein per ml, and 5 mM $Na_2S_2O_4$; (*b*) same as (*a*), but including an ATP-generating system to keep the concentration of Mg·ATP near 5 mM. The sample was quick frozen 45 sec after mixing. (*c*) same as (*b*), except that methylviologen (40 μM) and additional phosphocreatine (10 mM) were present, and the sample was incubated for 15 min before freezing. At this point the blue cast due to reduced methylviologen had disappeared. The amplifier gains for these spectra were 5× those of Fig. 2.

of reaction mixtures composed of *A. vinelandii* proteins, paralleling the experiments shown in Figs. 2 and 3, is depicted in Fig. 5. Inactivation of the nitrogenase system by O_2, in contrast to physiologically significant oxidation by substrates, yields denatured products with large signals at g = 4.3 and 2, as well as a transient complex of signals around g = 1.9 (12). Such signals were not observed in these experiments when the steps described to exclude O_2 were observed.

Electron transfers among nitrogenase components

The experiments described here refer to steady and equilibrium states of the system, and form a basis for kinetic studies with the freeze-quench technique and EPR measurements. However, from these and earlier observations one can propose a reasonable hypothesis about the order of partial reactions that occur during reduction of N_2. Because the signal from the MoFe protein (*a*) is present before reducing equivalents are added to the complete reaction system, (*b*) is suppressed during the steady state, and (*c*) reappears during reoxidation of the system, it is reasonable to suppose that it represents the oxidized MoFe protein, even as isolated in the presence of $Na_2S_2O_4$. The Fe protein from EPR evidence is strongly affected by the presence of Mg·ATP, and in fact binds Mg·ATP in the absence of the MoFe protein (19). The MoFe protein signal is not strongly affected by the Fe protein alone, but is suppressed by the Fe protein–Mg·ATP complex when $Na_2S_2O_4$ is present. Apparently, this reduced complex reduces the MoFe protein, and subsequent exhaustion of reductant leads to the disappearance of the Fe protein signal. In this respect, the Fe protein–Mg·ATP complex behaves like a plant-type ferredoxin, i.e., it gives a signal with average g-value below 2 in the *reduced* state, and no signal in the oxidized state (21). Because the complete system reduces protons, N_2, or other substrates only when accompanied by Mg·ATP hydrolysis (19, 20), the Fe protein–Mg·ATP complex may be a more powerful reductant than the Fe protein alone, and this accounts for the ability of the complex to reduce MoFe protein. Whether the energy released upon Mg·ATP hydrolysis is used in this way, or whether the Mg·ATP removes a purely kinetic inhibition from the interaction of the reduced Fe protein and the oxidized MoFe protein, is not established. In this regard one should note that the split signal near g = 4, from Fe protein–Mg·ATP (Fig. 3*b*), is absent from the spectrum of the complete system in the presence of excess reductant (Fig. 3*c*). This may indicate that *two* electron-transferring centers are active in the complex of Mg·ATP with Fe protein.

It is not known whether the oxidized Fe protein, which is very unstable in the absence of strong reductants, is reduced in the absence of Mg·ATP, nor whether ATP is bound to nitrogenase during the actual reduction of N_2, protons, or other substrates. The hydrolysis of ATP may occur at the substrate reduction step or during electron transfer from the Fe protein to the MoFe protein. It is not known how many electrons the Fe protein conveys to the MoFe protein per interaction. In earlier speculation, based on Mg·ATP and cyanide-binding experiments (19), in which the redox status of the components was not assessed, it was suggested that the Fe protein passes electrons to the MoFe protein, which in turn reduces substrates. The present evidence, the binding experiments (19), and the fact that dithionite oxidation and ATP hydrolysis are interdependent (20), suggest that the following events occur during nitrogen fixation:

(*i*) Mg·ATP binds to the reduced Fe protein. The EPR spectrum is substantially altered during this binding. Significant Mg·ATP hydrolysis does *not* occur as a result of this.

(*ii*) The reduced Fe protein will not reduce the MoFe protein, but the reduced Fe protein–Mg·ATP complex does reduce the MoFe protein.

(*iii*) The reduced MoFe protein and reduced Fe protein, in the presence of Mg·ATP, are reoxidized by substrates; this is apparent in the EPR spectra when the reductant is exhausted.

We think that these events, seen in limiting states of reaction mixtures, reflect molecular events during fixation of N_2.

We thank Professor H. Beinert for the use of his EPR facilities. This work was supported by the Public Health Service, through National Institutes of Health Grants GM-17170, GM-12394, AM-12153, and AI-00848, by a Career Development Award GM-10,236 (to W. H. O-J.), by the National Science Foundation Grant GB-483, and by the Graduate Research Committee of the University of Wisconsin.

1. Bulen, W. A. & LeComte, J. R. (1966) *Proc. Nat. Acad. Sci. USA* **56**, 979–986.
2. Burns, R. C., Holsten, R. D. & Hardy, R. W. F. (1970) *Biochem. Biophys. Res. Commun.* **39**, 90–99.
3. Shah, V. K., Davis, L. C. & Brill, W. J. (1972) *Biochim. Biophys. Acta* **256**, 498–511.
4. Mortenson, L. E. (1966) *Biochim. Biophys. Acta* **127**, 18–25.
5. Mortenson, L. E., Morris, J. A. & Jeng, D. Y. (1967) *Biochim. Biophys. Acta* **141**, 516–522.
6. Vandecasteele, J.-P. & Burris, R. H. (1970) *J. Bacteriol.* **101**, 794–801.
7. Tso, M.-Y. W., Ljones, T. & Burris, R. H. (1972) *Biochim. Biophys. Acta* **267**, 600–604.
8. Kelly, M. (1969) *Biochim. Biophys. Acta* **171**, 9–22.
9. Eady, R. R., Smith, B. E., Cook, K. A. & Postgate, J. R. (1972) *Biochem. J.* **128**, 655–675.
10. Davis, L. C., Shah, V. K., Brill, W. J. & Orme-Johnson, W. H. (1972) *Biochim. Biophys. Acta* **256**, 512–523.
11. Hardy, R. W. F., Burns, R. D. & Parshall, G. W., (1971) in *Bioinorganic Chemistry* (American Chemical Society, Washington, D.C.), pp. 219–247.
12. Dalton, H. & Mortenson, L. E. (1972) *Bacteriol. Rev.* **36**, 231–260.
13. Brintzinger, H. (1966) *Biochemistry* **5**, 3947–3950.
14. Palmer, G. (1967) in *Methods in Enzymology* eds. Estabrook, R. W. & Pullman, M. R. (Academic Press, New York), Vol. X, pp. 594–609.
15. Hansen, R. E., VanGelder, B. F. & Beinert, H. (1970) *Anal. Biochem.* **35**, 287–292.
16. Sweetser, P. B. (1967) *Anal. Chem.* **39**, 979.
17. Goa, J. (1953) *Scand. J. Clin. Lab. Invest.* **5**, 218–222.
18. Van de Bogart, M. & Beinert, H. (1967) *Anal. Biochem.* **20**, 325–334.
19. Bui, P. T. & Mortenson, L. E. (1968) *Proc. Nat. Acad. Sci. USA* **61**, 1021–1027.
20. Ljones, T. & Burris, R. H. (1972) *Biochim. Biophys. Acta* **275**, 93–101.
21. Palmer, G. & Sands, R. H. (1966) *J. Biol. Chem.* **241**, 253–254.